Development of Control System of the Single Phase Multi-Input Inverter for Microgrids

C. Ramonas[1], V. Adomavicius[1]
[1]*Department of Electric Energy Systems, Kaunas University of Technology, Studentu St. 48-205, 51367 Kaunas, Lithuania*
vytautas.adomavicius@ktu.lt

***Abstract*—Scheme of the small-scale microgrid inverter control system is investigated and described. The researched microgrid is intended for small-scale power users, which maximum capacity does not exceed 5 kW. Results of the control system research are presented. Method of mathematical modelling was used for researches of the system. The MATLAB/SIMULINK model was worked out for this purpose. The model was based on the SymPowerSystems library. The main target of the researches was active and reactive power control in the microgrid. The curves reflecting the possibility and quality of the independent active and reactive power control in the microgrid are presented and discussed.**

***Index Terms*—Microgrid, distributed power generation, control system, pulse inverters, DC-DC power converters.**

I. INTRODUCTION

Introduction of microgrids connected to the main power system paves the way to the improvement of power generation and supply technologies in many aspects. The traditional power system has one way power transmission from the generators to the power users, where the intermittent RES-based power sources also are integrated in the grid of the electric energy system and no matter where this unstable power will be consumed.

In the microgrids the energy generated by intermittent power plants mostly is consumed in the boundaries of microgrid and only surplus power can be supplied into the grid of power system. Bulk power consumption in the microgrids excludes existence of significant losses related with the power transmission and distribution over long distances as it happens in the traditional power system, because the generated energy mainly is consumed locally. In this way the microgrid has not significant impact to the power system operation when they are connected, because the main grid receives substantially less intermittent power in comparison with traditional power system. Besides this, introduction of microgrids has many other benefits making power supply by means of this technology more efficient, environmental friendly and more reliable [1]–[3].

Presently average capacity of already existing microgrids is about 1 MW; however there are many power users, which do not consume much energy, and bulk of their power demands can be met from the small-scale microgrids. Their maximum capacity usually does not exceed 5 kW. Usually this capacity is sufficient for majority of the one family houses.

Efficient operation of microgrid mostly depends on architecture of power generating and storage units, ratios of their installed rated powers and especially on the quality of control system operation. Results of researches of some power parameters control in the proposed small-scale microgrid are presented in this paper.

Manuscript received April 16, 2014; accepted August 15, 2014.

II. OBJECT OF INVESTIGATION

Object of investigation is control system of multi-input converter with common inverter and separate inputs designed for integration of various renewable energy power sources and power storage facilities operating in a small-scale microgrid. Simplified power conversion scheme of the small-scale microgrid based on this type multi-input inverter is shown in Fig. 1. The microgrid contains several (multi) primal usually unstable renewable power sources with DC-DC boost choppers connected to the common grid-connected inverter. Similar small-scale microgrid and its properties partially were explored in our previous papers [4], [5]. The presented converter topology provided with a proper control system is suitable to carry out the MPPT job taking into account renewable energy's instantaneous parameters of the exploited energy source separately and independently in every renewable power system included in the microgrid [6].

The mentioned above microgrid in general case may to have a number ("*n*") of DC voltage sources U_{si} connected to the corresponding DC boost choppers (DCCi) and the common one phase grid-connected inverter comprised of the transistors $V_1 \div V_4$ and diodes $V_{at1} – V_{at4}$. The DC choppers convert output DC voltages of the RES-based power sources to the DC voltages up to the values acceptable for the H-bridge grid-connected inverter. This last unit integrates the power received from the all mentioned above boost choppers DCCi and supplies the resulting power to the common bus of microgrid.

Figure 1 shows that such converter topology lets independent DCCi operation and control. Output voltages of the DC choppers are controlled by means of the PW modulation. Control systems of the RES-based power sources ensure the independent MPPT control and optimal control of every power source u_{si}.

As it is depicted in Fig. 1, all loads of the microgrid are united in the two equivalent loads.

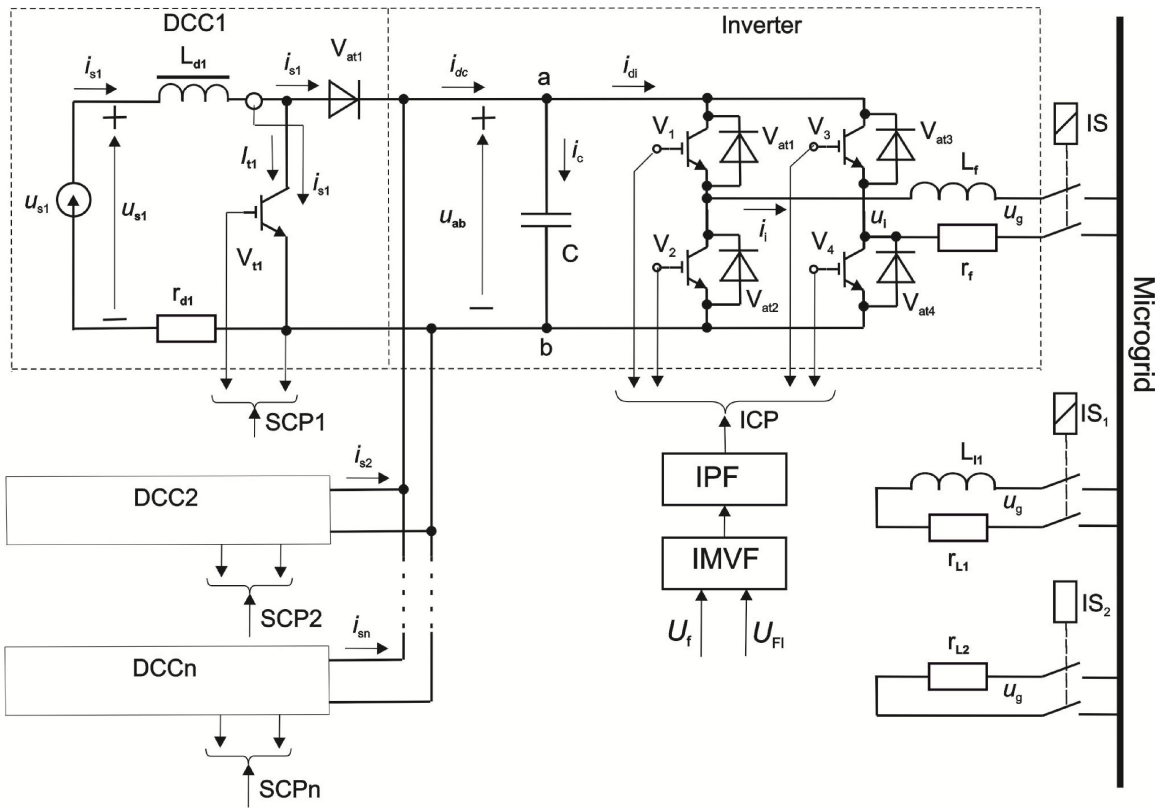

Fig. 1. Power circuits of the researched small-scale microgrid.

All reactive loads having inductive character are joined in one equivalent load with parameters of resistance r_{L1} and inductance L_{l1}. All purely active loads are joined in one equivalent load with parameter of resistance r_{L2}.

III. MATHEMATICAL EXPRESSIONS

The system has the DC part consisting of RES-based power sources with DC choppers and AC part consisting of single phase grid-tied inverter (Fig. 1). The RES-based power sources here (Fig. 1) are considered as the absolute DC voltage sources in order to simplify mathematical description of the system. Mathematical analysis of AC part of the system is more convenient when it is imagined as the d-q rotating frame. The Imaginary Circuit method suggested by R. Zhang [7] is used for conversion of the Real Circuit from the Cartesian coordinate system to the d-q rotating system. Thereby sinusoidal steady state operating point is turned into the DC operating point. The equivalent circuitry of the microgrid system for average values is shown in Fig. 2.

The Imaginary Orthogonal Circuit is introduced for AC part in this equivalent scheme. The components and parameters of this circuit are the same as in the Real Circuit. The variables of the system state U_I and I_I are similar to Real Circuit corresponding variables – they are only orthogonal to U_R and I_R.

Operation process of the DC chopper has two periods: the energy accumulating in the inductance L_{di} of the inductor (switch S_i is ON (S_i = 1)) and the energy passing to the inverter input (switch S_i is OFF (S_i = 0)). The duty cycle ¥ of the DC chopper indicates the energy accumulating interval and can be related with the chopper's operation frequency in this way

$$¥ = ² \times f_c = \frac{²}{Tc}, \tag{1}$$

where ² – the time period when switch S_i conducts, T_c – the period of chopping, f_{cc} – the chopper's operation frequency.

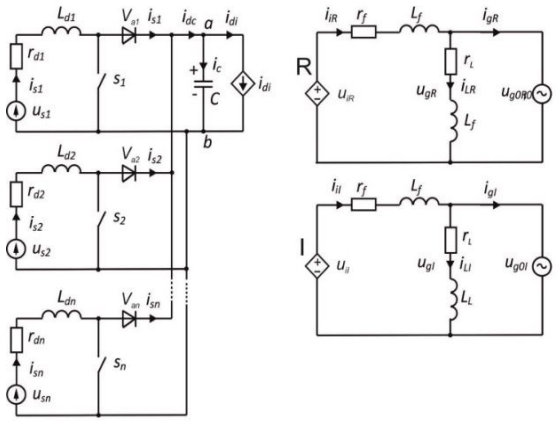

Fig. 2. The equivalent circuitry of the small-scale microgrid.

The equation for the current of the DC boost chopper state can be expressed as follows

$$\frac{di_{si}}{dt} = \frac{u_{si} - (1 - S_i)u_{ab}}{L_{di}} - \frac{r_{di}}{L_{di}} i_{si}. \tag{2}$$

Solution of the differential equation (2) gives the following result

$$i_{si} = \frac{u_{si} - (1 - S_i)u_{ab}}{r_{di}} \left(1 - e^{-\frac{r_{di}}{L_{di}}t}\right) + I_{si}(0)e^{-\frac{r_{di}}{L_{di}}t}. \tag{3}$$

The average value of the source current can be found from this equation

$$I_{si} = \frac{1}{T}\int_0^T i_{si}dt, \tag{4}$$

where T – the period of grid voltage; $I_{si}(0) = I_{min}$, when $T = 0$, or T_c and $I_{si}(0) = I_{max}$, when $T = \gamma T_c$.

The common average DC current can be determined from this equation

$$I_{dc} = \sum_{i=1}^{n} I_{si}. \tag{5}$$

The AC part of converter can be described as follows:

$$\begin{cases} \dfrac{di_i}{dt} = \dfrac{u_i - u_g}{L_f} - \dfrac{r_f}{L_f} i_i, \\ \dfrac{di_L}{dt} = \dfrac{1}{L_L} u_g - \dfrac{r_L}{L_L} i_L, \\ \dfrac{du_c}{dt} = \dfrac{1}{C}\left(i_{dc} - i_{di}\right), \\ U_{ab}(0) \cong \sqrt{2}\left(U_g + r_f i_i\right) = Uim, \\ u_{ab} = U_{ab}(0) + u_{dc}, \\ i_i - i_g - i_L = 0. \end{cases} \tag{6}$$

As it was mentioned above, we use the methodology of vector control [7] for a single-phase inverter of the microgrid (Fig. 1). Variables in the system of equations (6) in the Real Circuit can be related in this way

$$x_R = X_m \cos(\mu t + ¤). \tag{7}$$

Consequently, the same variables in Imaginary Orthogonal Circuit have to be expressed in this way

$$x_I = X_m \sin(\mu t + ¤). \tag{8}$$

The stationary Real and Imaginary variables to the synchronous rotating d-q reference frame are expressed by using this transformation matrix

$$T = \begin{bmatrix} \sin(\mu t) & -\cos(\mu t) \\ \cos(\mu t) & \sin(\mu t) \end{bmatrix}. \tag{9}$$

The variables in the rotating d-q frame become DC values as it is described in this equation:

$$\begin{bmatrix} x_d \\ x_q \end{bmatrix} = T \begin{bmatrix} x_R \\ x_I \end{bmatrix} = X_m \begin{bmatrix} \cos ¤ \\ \sin ¤ \end{bmatrix}. \tag{10}$$

According to this methodology, the matrix for inverse transformation from the d-q rotating frame to the stationary Real and Imaginary Circuit variables has this shape

$$T = \begin{bmatrix} \sin(\mu t) & \cos(\mu t) \\ -\cos(\mu t) & \sin(\mu t) \end{bmatrix}. \tag{11}$$

So, voltage of inverter output for the main harmonic can be expressed as follows

$$u_i = U_{im} \cos(\mu t + ¤_i). \tag{12}$$

Accordingly, inverter output voltage for Real and Imaginary Circuit can be expressed in the same way:

$$u_{iR} = U_{im} \cos(\mu t + ¤_i), \tag{13}$$

$$u_{iI} = U_{im} \sin(\mu t + ¤_i). \tag{14}$$

Applying the d-q rotating transformation to some of equations (6), which are necessary to build the block diagram of inverter control system operating in the d-q rotating frame, can be expressed by the following:

$$\frac{d}{dt}\begin{bmatrix} i_{id} \\ i_{iq} \end{bmatrix} = \begin{bmatrix} -\dfrac{r_f}{L_f} & \mu \\ -\mu & -\dfrac{r_f}{L_f} \end{bmatrix} \begin{bmatrix} i_{id} \\ i_{iq} \end{bmatrix} + \frac{1}{L_f}\begin{bmatrix} \left(u_{id} - u_{gd}\right) \\ \left(u_{iq} - u_{gq}\right) \end{bmatrix}, \tag{15}$$

$$\frac{d}{dt}\begin{bmatrix} i_{Ld} \\ i_{Lq} \end{bmatrix} = \begin{bmatrix} -\dfrac{r_L}{L_L} & \mu \\ -\mu & -\dfrac{r_L}{L_L} \end{bmatrix} \begin{bmatrix} i_{Ld} \\ i_{Lq} \end{bmatrix} + \frac{1}{L_L}\begin{bmatrix} u_{gd} \\ u_{gq} \end{bmatrix}. \tag{16}$$

The active and reactive power in the rotating frame can be described by well-known expressions:

$$P = u_d i_d + u_q i_q, \tag{17}$$

$$Q = u_q i_d - u_d i_q. \tag{18}$$

When the d-axis of the rotating frame is superposed with the grid's phase voltage u_g vector of the Real Circuit in the point of common connection (PCC), then $u_d = |U_{gm}|$ and $u_q = 0$. In this case (17) and (18) can be shortened:

$$P_{in} = \left|U_{gm}\right| i_{id}, \tag{19}$$

$$Q_{in} = -\left|U_{gm}\right| i_{iq}. \tag{20}$$

The DC voltage u_{ab} on input of the grid-tied inverter must to have wanted constant value. In the case when harmonics caused by switching are discounted and losses in the filter inductor resistance r_f and converter are not taken into consideration, AC and DC parts of inverter can be related as follows [8]

$$\left.\begin{array}{l} P = |U|\, i \\ |U| \cong mu \\ P = u\, i \end{array}\right\} \Rightarrow i = mi. \tag{21}$$

After this differential equation of the DC chain (Fig. 1) can be written in this way

$$C\frac{du_c}{dt} = i_{dc} - i_{di} = i_{dc} - m_a i_{id}. \tag{22}$$

Existence of a cross-coupling between *d-q* components, what is capable to make influence to the dynamics performance of the regulators [9], can be seen from (15). The output voltages for these circuits in the synchronous reference frame should be chosen as follows below in order to perform decoupled control of inverter currents:

$$\begin{cases} u_{id} = L_f\left(y_1 + \mu i_{iq}\right) + \left|U_{gm}\right|, \\ u_{iq} = L_f\left(y_2 - \mu i_{id}\right). \end{cases} \tag{23}$$

After this equations of the system (15) become invariant and can be expressed as follows:

$$\frac{d}{dt}\begin{bmatrix} i_{id} \\ i_{iq} \end{bmatrix} = -\frac{r_f}{L_f}\begin{bmatrix} 1 & 0 \\ 0 & 1 \end{bmatrix}\begin{bmatrix} i_{id} \\ i_{iq} \end{bmatrix} + \begin{bmatrix} y_1 \\ y_2 \end{bmatrix}. \tag{24}$$

As it follows from (19) and (20), the active and reactive inverted power can be controlled through i_d and i_q, respectively. The control rules (23) can be applied for inverter circuit by using current feedback loops defined as follows:

$$y_1 = \left(k_p + \frac{k_i}{s}\right)\left(i_{id}^* - i_{id}\right), \tag{25}$$

$$y_2 = \left(k_p + \frac{k_i}{s}\right)\left(i_{iq}^* - i_{iq}\right). \tag{26}$$

Applying Laplace transform and assuming that d-axis is aligned with the grid phase voltage u_g vector, the system of (16) can be transformed in this way:

$$\begin{cases} si_{Ld}(s) = \dfrac{1}{L_L}\left[-r_L i_{Ld}(s) + \mu i_{Lq}(s) + \left|U_{gm}\right|\right] + I_{Ld}(0), \\ si_{Lq}(s) = \dfrac{1}{L_L}\left[-r_L i_{Lq}(s) - \mu i_{Ld}(s)\right] + I_{Lq}(0). \end{cases} \tag{27}$$

Active and reactive power of the load can be expressed in this way:

$$P_L = \left|U_{gm}\right| i_{Ld}, \tag{28}$$

$$Q_L = -\left|U_{gm}\right| i_{Lq}. \tag{29}$$

The grid current in d-q reference frame can be expressed as follows:

$$\begin{cases} i_{gd}(s) = i_{id}(s) - i_{Ld}(s), \\ i_{gq}(s) = i_{iq}(s) - i_{Lq}(s). \end{cases} \tag{30}$$

After this active and reactive power of the grid can be determined by means of the following equations:

$$P_g = \left|U_{gm}\right| i_{gd}, \tag{31}$$

$$Q_g = -\left|U_{gm}\right| i_{gq}. \tag{32}$$

The grid voltage magnitude is determined in this way

$$U_{gm} = \sqrt{2}U_g, \tag{33}$$

where U_g – root mean square phase voltage of the grid.

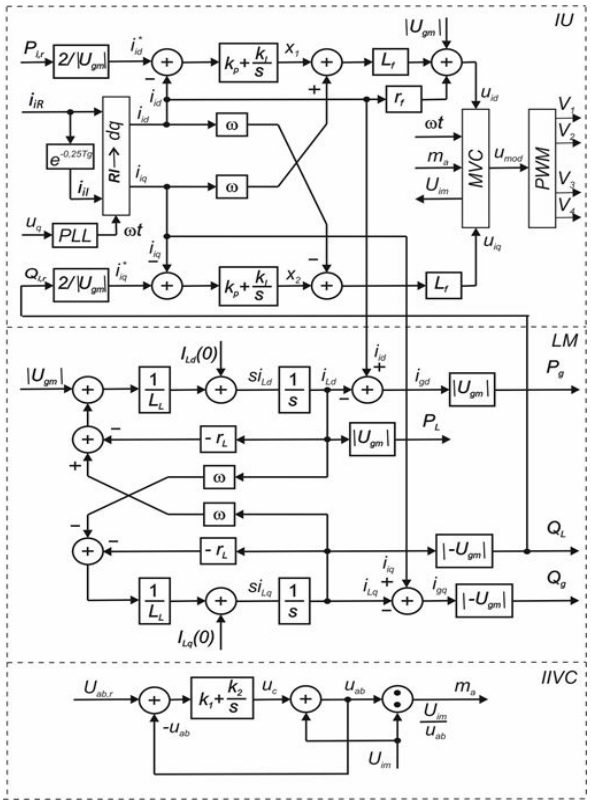

Fig. 3. Vector control diagram of single-phase grid-tied inverter.

Vector control diagram of single-phase grid-tied inverter is structured on basis of (15)–(33) and shown in Fig. 3. Structural diagram of the inverter *IU* is comprised of Real and Imaginary circuitries. Real and Imaginary components of the inverter current are transformed into rotating coordinate system d-q, where axis d is superposed with the vector of grid voltage u_g. This transformation converts sine type variables into permanent variables. In this case the methodology used for regulators design for the DC circuitries can be applied. The same regulators of PI type are used for the control of currents in the d-q coordinate system. Channels d and q are identical (cross-ties are removed by means of (23)) and therefore active and reactive inverted powers can be controlled independently: channel d controls the active power and channel q controls the reactive power. Modulation voltage control unit *MVC* forms sine type voltage of the necessary amplitude and phase, which is directed to the inverter control unit *PWM*. *MVC* unit also calculates amplitude of the inverter output voltage first harmonic U_{im}, which is passed to the DC regulator *IIVC*. Diagram of the microgrid load circuitry unit *LM* is designed in a similar way. Active and reactive powers of the load and inverter are calculated in this unit too.

The closed loop circuitry *IIVC* is developed on basis of PI

controller and is used in order to keep the DC voltage u_{ab} on a desirable value.

The reference value of DC voltage depends on the voltage of grid, on the inverted current and on the resistance of the filter and can be chosen in the boundaries

$$U_{abr} = (1.2 \div 1.8) \times U_{gm}. \quad (34)$$

This unit calculates the modulation index m_a, which is passed to the modulation voltage controller *MVC* of the inverter control system (Fig. 3).

IV. MATHEMATICAL MODEL OF THE MICROGRID

Model diagram of the microgrid is shown in Fig. 4. It includes the PV and WT sources, the common single-phase grid-tied inverter, the grid, the load, the filter and the active/reactive powers measurement units. The outputs of the power sources are DC voltages. Each power source consists of the resistance R_d and the inductance L_d of the inductor, the transistor V_t and the diode V_{at}. The control system of each source is equipped with MPPT function. The unit U_{abr} refers the inverter's input voltage.

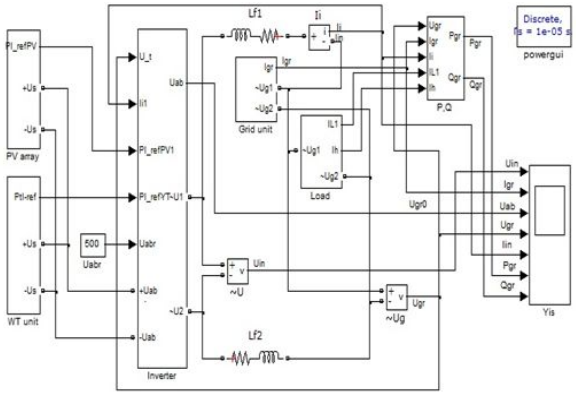

Fig. 4. Model diagram of the researched microgrid system.

Model of the vector control system of inverter is depicted in Fig. 5. It contains the single-phase PLL part, the inverter part with modulation voltage calculator (Mod_voltage), the load part with the devices for measurement of the active and reactive powers operating in the microgrid.

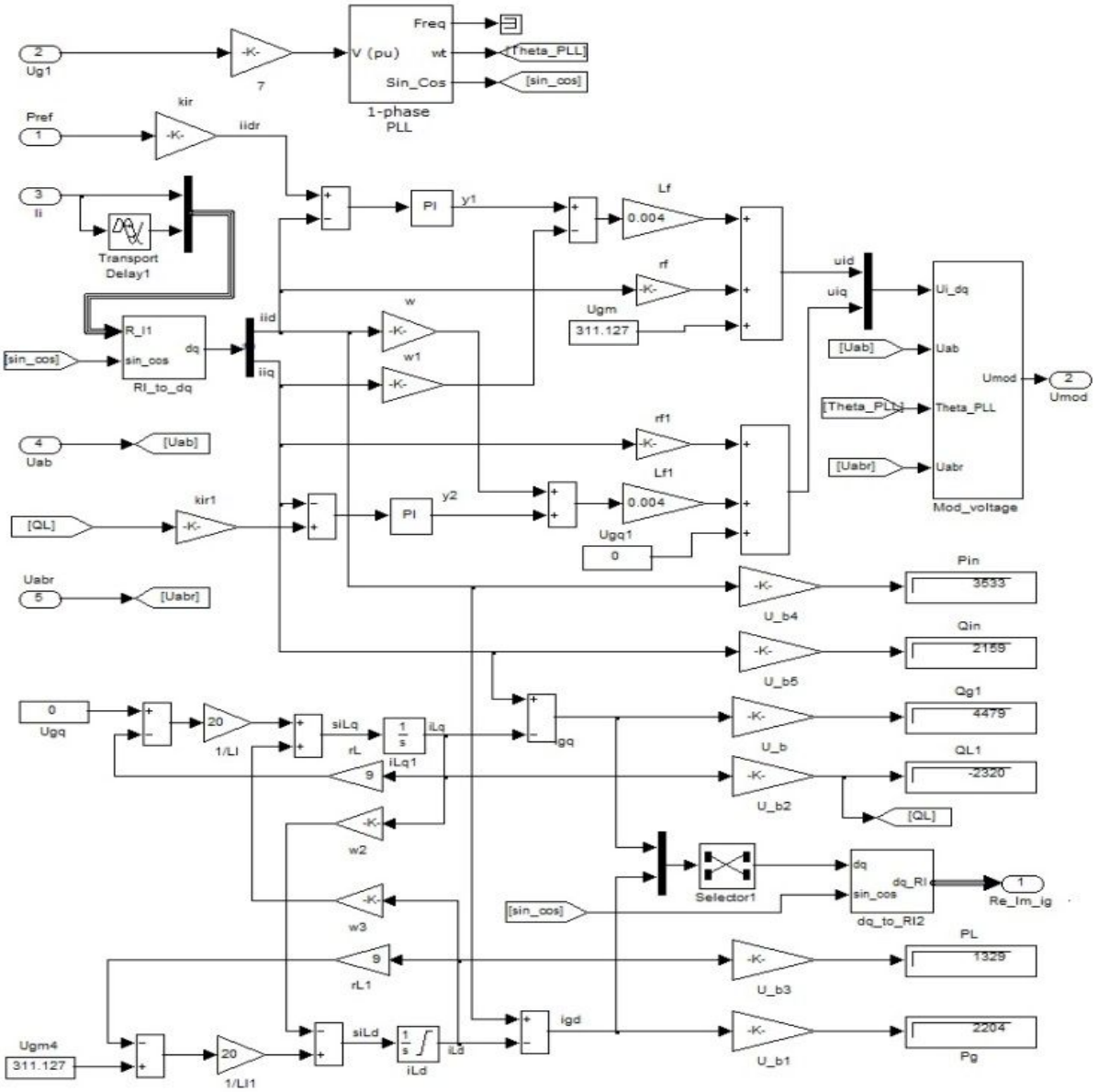

Fig. 5. Model diagram of the inverter vector control system.

Unit "Mod voltage" has regulator of the DC voltage connected to the terminals of inverter input. Unit "RI_to_dq" transforms the Real and Imaginary components of the inverter current into the rotating system of coordinate d-q and unit "dq_to_RI" performs the reciprocal transformation of grid current i_g from the system of coordinate d-q into the stationary Cartesian system of coordinate.

V. RESULTS OF THE RESEARCH

Multi-input inverter has specific requirements for control system. Therefore some modifications for calculation of the inverter modulation voltage and working out of the inverter input voltage control system were introduced in comparison with methodology of traditional control system designing. Control systems performing the MPPT function and researched in previous investigations of authors [5] were used for the small-scale WT and PV power source control.

Research of the inverter and microgrid control system operation is performed by means of digital simulation. Results of vector control system application possibility for multi-input inverter are shown in Fig. 6 and Fig. 7.

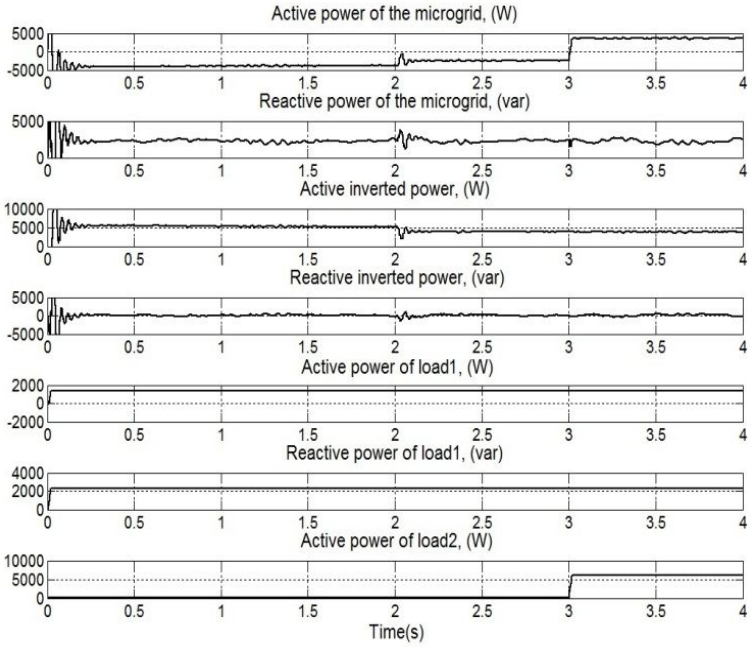

Fig. 6. Curves of the active and reactive powers in the system versus time at the jumps of solar irradiance (E jump from 600 to 400 W/m^2, at t = 2 s) and second load (load R_{L2} = 8 Ω was switched on after 3 s additionally to the operating load R_{L1} = 9 Ω, L_{L1} = 0,05 Hn) for the case when $Q \approx 0$.

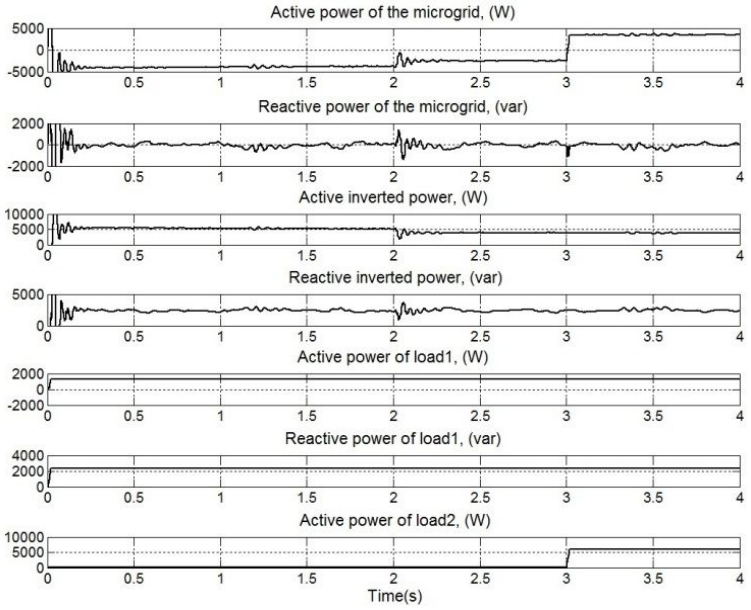

Fig. 7. Curves of the active and reactive powers in the system versus time at the jumps of solar irradiance (E jump from 600 W/m^2 to 400 W/m^2, at t = 2 s) and second load (load R_{L2} = 8 Ω was switched on after 3 s additionally to the operating load R_{L1} = 9 Ω, L_{L1} = 0,05 Hn) for the case when $Q \approx 0$.

Investigations of inverter vector control system operation confirmed the possibility of independent active and reactive power control in the output of inverter. Grid-tied inverter can operate as the active power supplier to the microgrid loads and compensator of the reactive power of the loads simultaneously. In the Fig. 6 is shown the case of inverter operation when it supplies the active power to the load of microgrid and the reactive power in output of the inverter is

equal to zero. It shows the fourth curve of the figure (from above). The first curve shows variation of the active power in the microgrid after the jump variations of the generated power and the load power in the microgrid. Initially the power is negative and this means that microgrid's loads do not consume all generated power and therefore the surplus power is supplied into the grid. The generated power of the PV source decreases after the jump of irradiance from 600 W/m^2 to 400 W/m^2 at the time mark 2 s and the active load in microgrid increases at the time mark 3s. After this the total generated power in the microgrid becomes insufficient for feeding the switched on loads and therefore deficient power is being taken from the grid. At this moment the power curve changes its sign from negative to positive. The inverter supplies only the active power to the microgrid and therefore reactive power is being supplied to the load from the grid (see the second curve from the top). Consumer of the reactive power is the first load (the sixth curve).

Another case of inverter operation is presented in Fig. 7, when it supplies not only active but also reactive power into the microgrid. In this case reference of the reactive power has the value necessary for compensation of the reactive power taken by the first load from the grid. The second curve (from above, Fig. 7) shows that reactive power of the microgrid is kept close to zero.

So, only active power is supplied into the grid, while reactive power of the first load is taken from the inverter. It shows the fourth curve. Summarizing analysis of the received curves it can be noted that inverter's vector control system operates correctly.

V. CONCLUSIONS

Operation of the microgrid consisting of the PV and WT energy sources, mutual multi-input inverter and two equivalent loads was researched. Results of the research show correct operation of vector control system adapted for the single-phase multi-input inverter. It was found that vector control system allows independent control of the active and reactive power in the inverter output.

It was proved that control of reactive power allows achieving of only the active power in output of the inverter or the reactive power as well, which is necessary for the compensation of the reactive power taken by the load of microgrid. In this case only the active power can be supplied from the microgrid into the grid of the main power system.

It was also proved that interchange of active and reactive power between the microgrid and the main grid is easily possible: the surplus of electricity produced in the microgrid can be supplied into the main electric grid and vice versa.

In general, results of this research allow supporting the idea that properly controlled microgrid can operate as the interactive load for the main grid of the power system. It can operate as power generator and support the main grid when it is reasonable. It also can function as load in regard of the main power system taking the deficient power from the main grid for feeding microgrid's loads when it is necessary.

REFERENCES

[1] F. Katiraei, R. Iravani, N. Hatziargyriou, A. Dimeas, "Microgrids management. Controls and operation aspects of microgrids", *IEEE Power and Energy Magazine*, 2008, pp. 54–65. [Online]. Available: http://dx.doi.org/10.1109/MPE.2008.918702

[2] A. Ravichandran, P. Malysz, S. Sirouspour, A. Emadi, "The critical role of microgrids in transition to a smarter grid: a technical review", *IEEE Transportation Electrification Conf. and Expo (ITEC)*, Detroit, MI, 2013, pp. 1–7. [Online]. Available: http://dx.doi.org/10.1109/ITEC.2013.6573507

[3] T. Deveikis, R. Miliune, E. V. Nevardauskas, "Reliability of divided small electric energy system", *Elektronika ir Elektrotechnika*, vol. 19, no. 10, pp. 21–24, 2013.

[4] C. Ramonas, V. Adomavicius, "Research of the converter control possibilities in the grid-tied PV power plant", *Elektronika ir Elektrotechnika*, vol. 19, no. 10, pp. 37–40, 2013.

[5] C. Ramonas, V. Adomavicius, "Grid-tied converter with intermediate storage chain for multipurpose applications", *Elektronika ir Elektrotechnika*, no. 7, pp. 15–20, 2011.

[6] C. Ramonas, V. Adomavicius, "Impact of DC/DC converter parameters on operation of solar power conversion system", in *Proc. of the 6th Int. Conf. on Electrical and Control Technologies (ECT)*, 2011, pp. 321–324.

[7] R. Zhang, M. Cardinal, P. Szczesny, M. Dame, "A grid simulator with control of single-phase power converters in D-Q rotating frame", in *Power Electronics Specialists Conf.*, 2002, vol. 3, pp.1431–1436.

[8] N. Mohan, T. M. Undeland, W. P. Robbins, *Power Electronics: Converter, Applications and Design*. New York: John Wiley & Sons, 2003, p. 802.

[9] D. N. Zmood, D. G. Holmes, G. H. Bode, "Frequency-domain analysis of three-phase linear current regulators", *IEEE Transactions on Industry Applications*, vol. 37, no. 2, 2001, pp. 601–610. [Online]. Available: http://dx.doi.org/10.1109/28.913727